JCTC Journal of Chemical Theory and Computation

Article

pubs.acs.org/JCTC

Macromolecular Stabilization by Excluded Cosolutes: Mean Field Theory of Crowded Solutions

Liel Sapir and Daniel Harries*

Institute of Chemistry and The Fritz Haber Research Center, The Hebrew University, Jerusalem 91904, Israel

Supporting Information

ABSTRACT: We propose a mean field theory to account for the experimentally determined temperature dependence of protein stabilization that emerges in solutions crowded by preferentially excluded cosolutes. Based on regular solution theory and employing the Flory–Huggins approximation, our model describes cosolutes in terms of their size, and two temperature-dependent microscopic parameters that correspond to macromolecule-cosolute and bulk solution interactions. The theory not only predicts a "depletion force" that can account for the experimentally observed stabilization of protein folding or association in the presence of excluded cosolutes but also predicts the full range of associated entropic and enthalpic components. Remarkably, depending on cosolute identity and in accordance with experiments, the theory describes entropically as well as enthalpically dominated depletion forces, even those *disfavored* by entropy. This emerging depletion attraction cannot be simply linked to molecular volumes. Instead, the relevant parameter is an effective volume that represents an interplay between solvent, cosolute, and macromolecular interactions. We demonstrate that the apparent depletion free energy is often accompanied by significant yet compensating entropy and enthalpy terms that, although having a net zero contribution to stabilization, can obscure the underlying molecular mechanism. This study underscores the importance of including often-neglected free energy terms that correspond to solvent-cosolute and cosolute-macromolecule interactions, which for most typical cosolutes are expected to be temperature dependent. We propose that experiments specifically aimed at resolving the temperature-dependence of cosolute exclusion from macromolecular surfaces should help reveal the full range of the underlying molecular mechanisms of the depletion force.

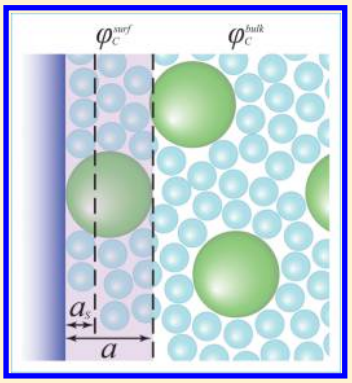

1. INTRODUCTION

The preferential exclusion of added solutes (or cosolutes) from macromolecular or colloidal interfaces in solution mediates an important form of effective attraction between these interfaces.[1] This "depletion force" has been shown to impact the stability of numerous solvated colloids and macromolecules and can direct their association and assembly.[2] Specifically, protein stability in the living cell is more easily maintained in the presence of excluded cosolutes that shift the protein folding equilibrium toward the folded, more compact state. Many osmolyte cosolutes, for example, are preferentially excluded from proteins, hence forming an extensive molecular "catalogue" used by organisms to impart increased cellular stability in face of external stress, thereby helping to sustain proteostasis.[3−6]

The net exclusion (or inclusion) of cosolutes from macromolecular surfaces is often quantified using the preferential hydration coefficient, Γ_W. Any association of macromolecules in the presence of cosolutes and subsequent burial of macromolecular interfaces incurs a change in preferential hydration, $\Delta\Gamma_W$. As dictated by the Gibbs adsorption isotherm,[7] for low cosolute concentrations the change in free energy accompanying the burial of macromolecular interfaces with osmotic pressure, Π, scales as the change in preferential hydration, $\Gamma_W = m_W(\partial\Delta G/\Delta\Pi)$, where m_W is the molality of the solvent. For excluded cosolutes that act to promote surface burial, $\Delta\Gamma_W < 0$. Conversely, in solutions containing cosolutes that are included at the interface, $\Delta\Gamma_W > 0$. An alternative (yet related) quantitative measure of cosolute action is the *m*-value, defined as the slope of ΔG with cosolute *molar* concentration.[8] A negative *m*-value implies that the cosolute is a stabilizer, whereas $m > 0$ characterizes denaturants.

In contrast to the thermodynamic formulation, the underlying molecular mechanisms that lead to the cosolute effects are still under debate. Clearly, however, the physical origin of $\Delta\Gamma_W$ is necessarily related to the effective interaction between cosolute and the macromolecular interface.[9−11] Moreover, according to the entropy–enthalpy compensation theorem, it can be shown that all other interactions within the solution do not directly contribute to the free energy changes imposed by cosolute.[12−15] It follows that the effective interaction between cosolute and macromolecule is key in deciphering cosolute action.

By considering cosolutes interacting with colloids exclusively through hard-core repulsions, Asakura and Oosawa[16,17] were first to afford a molecular model for the depletion attraction. Thus, a link was established between the depletion attraction to

Received: March 18, 2015
Published: May 20, 2015

DOI: 10.1021/acs.jctc.5b00258
J. Chem. Theory Comput. 2015, 11, 3478−3490

the entropic gain associated with the reduced cosolute-excluding volume upon macromolecular association. Importantly, this link predicts a stabilization energy that is linear in cosolute concentration and that also scales as cosolute size. A refined mechanism based on similar approaches was later applied to describe stabilization of protein folding and associations by excluded cosolutes or "crowders".[18−20]

Since the underlying molecular interactions considered in the Asakura−Oosawa model are athermal, the predicted depletion effect is purely entropic. Interestingly, for cosolute action on proteins this important prediction is experimentally found in only a few examples (see, e.g. ref 21). Rather, many experiments suggest that this stabilization also includes enthalpic contributions.[22−34] The molecular underpinnings for these observations must be related to interactions absent from the Asakura and Oosawa model, pointing specifically to effective cosolute-macromolecule interactions that go beyond hard-core.[35] These effective interactions arise from the collective action of all the intermolecular interactions between all solution components.

Molecularly large cosolutes such as polyethylene glycol (PEG) and in some cases dextran often induce an entropically dominated depletion force that is mitigated by an unfavorable (destabilizing) enthalpy.[22−24,28−33,36] The discrepancy between experiments and the Asakura−Oosawa model becomes even more prominent for osmolytes, such as trehalose and sorbitol, which have been unequivocally shown in experiments to induce *enthalpically dominated* depletion forces accompanied by an *entropic penalty*.[25,30,31] Surprisingly, even large polymeric macromolecular crowders, such as dextran, can induce such enthalpically driven entropically costly depletion forces.[34]

The deviations from the Asakura−Oosawa model have been rationalized by more recent models that accounted for interactions beyond hard-core. It was shown, for example, that unlike "soft" (or "chemical") attractions that weaken the induced depletion attraction,[22,23,33,36−43] "soft" repulsions can enhance it.[11,43−48] If the hard-core cosolute-macromolecule interaction is augmented by an additional "soft" repulsion, an enthalpically driven depletion force can emerge.[43] If, moreover, the "soft" repulsion shell is temperature-dependent, so that it is entropically attractive and enthalpically repulsive, this repulsion can even induce depletion forces that are dominated by an enthalpy that is large enough to overcome a disfavorable entropy.[11]

By using a solution theory that includes explicit interactions in the ternary macromolecule-solvent-cosolute system at the mean field level, in this study we show how effective cosolute-macromolecule attractions and repulsions emerge from the microscopic interactions. Moreover, we show that these temperature dependent cosolute-macromolecule interactions can naturally lead to enthalpically dominated depletion forces. The simple mean field theory of cosolute solutions (MFC) that we formulate here considers cosolute and solvent with free energy terms that describe the components' mixing in the presence and absence of macromolecular interfaces. With only a small number of molecular phenomenological parameters, the theory can account for the wide range of experimentally observed changes in free energy following cosolute addition. An important prediction is that temperature-dependent interactions terms acting both in the bulk solution and at the macromolecular interfaces are crucially important and often dominate the overall cosolute effect.

We start by presenting the theoretical model. We then use the model to discuss several limiting cases: first, those corresponding to previous models and, then, additional cases that extend their scope. We follow by comparing the model results with available experiments. Although the theory is able to fit experiments well, our aim here is primarily to demonstrate the necessity for explicitly including free energy (rather than purely enthalpic) microscopic parameters in the model. We end with conclusions and suggest that future experiments directed at resolving the molecular level phenomenological parameters could potentially allow a more complete understanding of the molecular mechanism of the excluded cosolute effect.

2. MODEL

We consider an extended macromolecular surface with total surface area A, representing the solvent accessible surface area of a solvated macromolecule. Many macromolecular processes, including protein folding and protein−protein interactions, are associated with reduced solvent accessible surface area due to partial protein "surface burial". The contribution of the interactions between associating interfaces and solution components can, therefore, be discussed in terms of the free energy change, ΔF_0, associated with this reduction in A following the macromolecular process. The addition of cosolute to the solution at some cosolute concentration changes the free energy of association to a new value ΔF_C. The change in association free energy upon cosolute addition, $\Delta\Delta F = \Delta F_C - \Delta F_0$, can be further dissected into its entropic and energetic components, $T\Delta\Delta S$ and $\Delta\Delta E$, respectively.

We shall consider surfaces immersed in a binary mixture, consisting of N_S^{bulk} solvent (S) molecules and N_C^{bulk} cosolute (C) molecules. The theory can easily be extended to account for additional cosolute species in solution. Following the Bragg-Williams mean field theory, the solution is treated within the framework of a 3-dimensional lattice. Each solvent particle occupies one lattice site, while each cosolute molecule occupies a volume of υ lattice sites.

When a macromolecular interface is introduced into solution, the binary mixture is perturbed, so that two domains form, Figure 1. First, the "*surface domain*" is composed of M^{surf} lattice sites, where $M^{surf} = N_S^{surf} + \upsilon N_C^{surf}$. The cosolute and solvent volume fractions in this domain are $\varphi_C^{surf} = \upsilon N_C^{surf}/M^{surf}$ and $\varphi_S^{surf} = N_S^{surf}/M^{surf}$, respectively. The extent of the surface domain, M^{surf}, represents the volume of solution that is directly affected by the presence of the interface (as we discuss below) and is set by

$$M^{surf} = Aa \tag{1}$$

where $a = \upsilon^{1/3}$ defines the typical linear dimension of the cosolute molecule, see Figure 1. The remainder of solution is considered to comprise the second, *"bulk domain"* composed of M^{bulk} lattice sites, where $M^{bulk} = N_S^{bulk} + \upsilon N_C^{bulk}$, with corresponding cosolute volume fraction $\varphi_C^{bulk} = \upsilon N_C^{bulk}/M^{bulk}$ and solvent volume fraction $\varphi_S^{bulk} = N_S^{bulk}/M^{bulk}$. In the following, we consider a surface domain that is much smaller than the bulk domain, implying $M^{surf}/M^{bulk} \to 0$. We note that within the lattice model the volume fraction is proportional to the molarity, M, since $\varphi_C = MN_{AV}\upsilon\bar{v}_S$. Here, N_{AV} is the Avogadro number, and $\bar{v}_S$ is the partial molar volume of the solvent. In the low concentration regime, the volume fraction also scales linearly with molality, m, because $\varphi_C = M\upsilon Mw_S/1000$, where Mw_S is the molar weight of the solvent.

DOI: 10.1021/acs.jctc.5b00258
J. Chem. Theory Comput. 2015, 11, 3478−3490

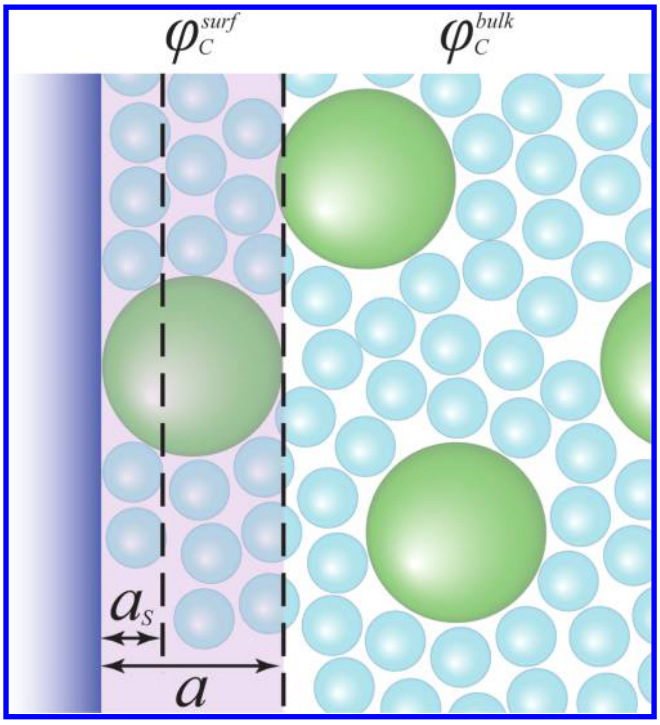

Figure 1. Schematic of the model system, comprising the surface domain and the bulk domain with cosolute (in green) volume fraction φ_C^{surf} and φ_C^{bulk}, respectively. The surface domain (pale pink background) extends a distance a away from the macromolecular surface (in blue). The volume in which particles can directly interact with the macromolecule through short-ranged interactions is of width $a_S = 1$ corresponding to the solvent (in cyan) linear dimension.

Next, we describe the mean field (MFC) free energy functional associated with each of the two domains. Minimization of the total free energy with respect to the composition in the bulk and surface domains leads to the equilibrium condition and subsequently allows us to calculate all the relevant thermodynamic properties.

2.1. Free Energy of the Bulk Domain. To model regular solutions that are mixtures of particles of unequal size, ranging from small (e.g., osmolytes) to large (e.g., polymers), we employ the Flory–Huggins (FH) approximation.[49−53] The FH free energy of mixing of solvent and cosolute in the bulk domain with respect to the pure, unmixed components is

$$\frac{\beta \Delta F_{bulk}}{M^{bulk}} = \phi_S^{bulk} \ln \phi_S^{bulk} + \frac{1}{\upsilon}\phi_C^{bulk} \ln \phi_C^{bulk} + \chi \phi_S^{bulk}\phi_C^{bulk} \tag{2}$$

where $\beta = (kT)^{-1}$, k is Boltzmann's constant, and T is the temperature. The first two terms in eq 2 correspond to the ideal FH mixing entropy, which takes into account in an approximate way the size disparity between mixed particles. The last term corresponds to nonideal mixing. In this expression, χ is the "mixing parameter", which is usually defined as $\chi = -z\beta\omega/2$, with $\omega = \omega_{SS} + \omega_{CC} - 2\omega_{SC}$, where ω_{ij} is the interaction energy between two near-neighbor lattice sites ($i,j = C,S$) occupied by cosolute (C) or solvent (S), respectively. Finally, z is the lattice coordination number.

While ω can be dominated by energetic terms, in the most general case it should be understood as an interaction *free energy* or more precisely as the difference in free energy between "reactants" and "products" in the hypothetical process ("reaction") $2SC \rightarrow SS + CC$. In the following, we define $\omega = \omega_E - T\omega_{TS}$, where ω_E and ω_{TS} are the energetic and entropic components of ω, which are themselves assumed to be independent of temperature. Hence, the nonideal mixing parameter becomes an effective free energy of interaction

$$\chi = -\frac{1}{2}z\beta\omega_E + \frac{z\omega_s}{2k} = \chi_E - \chi_{TS} \tag{3}$$

where χ_E and χ_{TS} are the energetic and entropic components of χ, respectively. Although treating χ as a free energy does not affect the expression for the free energy of mixing, eq 2, it does modify the relative contributions of mixing energy and entropy.

2.2. Free Energy of the Surface Domain. Similarly to the bulk domain, the part of solution residing within the surface domain is treated as a FH mixture but with two important modifications. First, we introduce an explicit interaction between cosolute and the macromolecular interface. This interaction is assumed to be short-ranged, so that it impacts only the first layer of lattice sites near the macromolecular surface (of width $a_S = 1$), which is in direct contact with the surface. This interaction leads to a total free energy contribution $\Delta F_{surf,excess}$, defined as

$$\beta \Delta F_{excess}^{surf} = \frac{1}{a} M^{surf} \varepsilon \phi_C^{surf} \tag{4}$$

where the division by a signifies that only the cosolute part residing in the first layer contacts the macromolecule (see Figure 1). In this expression, ε is the interface-cosolute interaction parameter defined per cosolute lattice site.

Analogously to the mixing parameter, χ, the parameter ε represents the free energy difference for replacing a solvent lattice unit at the interface with a cosolute lattice unit. Again, also $\varepsilon = \varepsilon_E - \varepsilon_{TS}$ should be understood to be a free energy that can be dissected into energetic, ε_E, and entropic, ε_{TS}, terms. With analogy to the transfer model paradigm and the description of cosolute effects as made from contributing interactions related to different macromolecular surface area types,[54−60] in cases where the surface consists of patches of chemically distinct moieties (as typical for proteins) the total surface free energy can be considered as a weighted sum of the contributions of all patches, each with its own ε. For simplicity, we shall consider here uniform surfaces with only one value of ε.

The second modification addresses the altered mixing entropy of cosolute close to the interface. Since the cosolute is generally larger than the solvent (say water), there exists a layer around the surface that is inaccessible to cosolute by virtue of steric size-exclusion alone. Because the cosolute's center of mass is excluded from entering a certain volume enveloping the interface, the expression for the mixing entropy of the solution within the surface domain is modified with respect to that in the bulk.

We define M^{mixed} as the number of surface-domain lattice sites that include all cosolute sites as well as any sites accessible to the cosolute within a distance of $a/2$ away from the surface. This number is smaller than M^{surf} for any $a > a_S$. We use an approximate expression for the fraction of sites within this "mixed" domain, which exactly recovers the size dependence at the limits of small and large cosolutes, as follows:

$$\frac{M^{mixed}}{M^{surf}} = 1 - \frac{1}{2}\left(1 - \frac{1}{a}\right)(1 - \phi_C^{surf}) \tag{5}$$

DOI: 10.1021/acs.jctc.5b00258
J. Chem. Theory Comput. 2015, 11, 3478−3490

Specifically, this ratio is 1 for $\upsilon = 1$ (cosolute and solvent of equal sizes) and equals 1/2 for molecularly large cosolutes present at low concentrations. The effective volume fraction of cosolute in this "mixed" subdomain is $\varphi_C^{surf,mixed} = \upsilon N_C^{surf}/M^{mixed}$. This subdivision of the surface domain defined by eq 5 is somewhat analogous to the introduction of the Stern layer in mean field electrostatic theories.[61,62] Here, it acts to include steric repulsion between cosolute and macromolecular interface that is of the order of the cosolute's molecular size and to effectively limit the cosolute's distance of closest approach to the interface.

The total free energy of mixing in the surface domain is then given by

$$\beta\Delta F_{surf} = M^{mixed}\left(\phi_S^{surf,mixed}\ln\phi_S^{surf,mixed} + \frac{1}{\upsilon}\phi_C^{surf,mixed}\ln\phi_C^{surf,mixed}\right) + M^{surf}\chi\phi_S^{surf}\phi_C^{surf}\left(1 - \frac{1-f}{a}\right) + \frac{1}{a}M^{surf}\varepsilon\phi_C^{surf} \quad (6)$$

The first part of eq 6 corresponds to the ideal mixing at the "mixed" surface domain. The first term in the second line describes the nonideal mixing contribution, where we account for changes in the possible number of neighbors a cosolute particle can have near the surface. The parameter that rescales the number of neighbors is f. Motivated by all-atom molecular dynamics simulations of sorbitol,[63] where we have found that typically $f \approx 1$, in the following we set $f = 1$, unless otherwise stated. As will be discussed further, the rescaling of f can also be regarded as a rescaling of χ near the surface in comparison to its value in the bulk, accounting for possible surface modified mixing free energy.

In order to determine the free energy gain following surface burial (viz., the excess free energy of solution at the macromolecular interface), the equilibrium condition is determined by taking the variation $\delta\Delta F_{system}/\delta N_C^{surf} = 0$, at a given concentration of cosolute in the bulk. The result of this minimization leads to the adsorption isotherm of cosolute on the surface in terms of φ_C^{surf} *versus* φ_C^{bulk}. Practically, we determine the adsorption isotherm numerically by solving the equilibrium condition in terms of the components' chemical potentials:

$$\mu_C^{surf} - \mu_C^{bulk} - \upsilon(\mu_S^{surf} - \mu_S^{bulk}) = 0 \quad (7)$$

The chemical potential μ_i of each component i is derived using the definition

$$\mu_i = \left(\frac{\partial F}{\partial N_i}\right)_{\beta,N_{i\neq j}} \quad (8)$$

2.3. Changes in Thermodynamic Quantities upon Macromolecular Surface Burial. Given a state of solution equilibrium in the presence of the macromolecular surface, we next calculate the changes in thermodynamic quantities upon burial of that interface. Within the model, this surface burial represents processes such as protein folding and macromolecular association. Importantly, the process involves the "release" of cosolute and solvent particles that were previously associated with the surface domain and their subsequent mixing with those in the bulk domain. Using eq 2, we calculate the change in free energy of the mixture upon surface burial, $\Delta F_{system}^{final}$. Subsequently, we calculate the corresponding changes in the different state functions upon cosolute addition: the change in mixing free energy per surface area, $\Delta\Delta F/A$, the energy, $\Delta\Delta E/A$, and the entropy, $\Delta\Delta S/A$, where $\Delta\Delta$ represents the differences in quantities with respect to the cosolute-free solution. The entropy was calculated by considering the temperature dependence of the free energy, so that $T\Delta\Delta S = \beta(\partial\Delta\Delta F/\partial\beta)$.

As discussed in the Introduction, the magnitude of stabilization or destabilization is quantified by the change in preferential hydration, $\Delta\Gamma_W$,[10,25,64,65] which in the following we designate $\Delta\Gamma$ for short. Since the lattice model is incompressible, so that $\Delta(PV) = 0$ (where P and V are the system pressure and volume, respectively), the enthalpic and energetic changes of any process are necessarily identical. Thus, $\Delta\Gamma$ becomes

$$\frac{\Delta\Gamma}{A} = -\frac{\partial(\Delta\Delta F/A)}{\partial\mu_S} = \frac{\partial(\Delta\Delta F/A)}{\bar{\nu}_S\partial\Pi} \quad (9)$$

Moreover, using eq 8 the expression for the osmotic pressure, Π, is

$$\Pi(\phi_C^{bulk})\bar{\nu}_S = \mu_S(\phi_C^{bulk} = 0) - \mu_S(\phi_C^{bulk}) = -kT\left[\ln(1-\phi_C^{bulk}) + \phi_C^{bulk}\left(1 - \frac{1}{\upsilon}\right) + \chi(\phi_C^{bulk})^2\right] \quad (10)$$

An alternative method to calculate $\Delta\Gamma$ is based on counting the number of cosolute and solvent molecules around the surface and in the bulk.[1,66] In our model this method allows for an easy evaluation of $\Delta\Gamma$, since the size of the surface domain is well-defined through the ratio of a and a_S. It follows that the change in preferential hydration coefficient is directly related to the cosolute adsorption isotherm through

$$\frac{\Delta\Gamma}{A} = -a\phi_S^{surf}\left(1 - \frac{\phi_C^{surf}}{\phi_S^{surf}}\frac{\phi_S^{bulk}}{\phi_C^{bulk}}\right) \quad (11)$$

where φ_S^{surf} and φ_C^{surf} are the equilibrium values after free-energy minimization, derived using eq 7.

3. RESULTS AND DISCUSSION

So far, we have formulated the MFC for cosolutes, as characterized by their size, υ, the interaction with the solvent, defined by χ and χ_{TS}, and the interaction with the surface, ε and ε_{TS}. In this section, we describe how these cosolute-specific microscopic parameters determine each cosolute's impact on the association of macromolecules or more generally the burial of interacting interfaces. In so doing, we recover some of the well-known limits of the cosolute effect, as well as present new predictions that emerge from the model.

3.1. The Asakura−Oosawa Limit. It is useful to first examine the MFC in the limit of the Asakura and Oosawa model (AOM).[16,17] In the AOM the interaction of cosolutes with the surface is entirely steric and all other interactions are absent, so that $\varepsilon = \varepsilon_{TS} = 0$. Also, since Asakura and Oosawa considered an ideal solution, the mixing parameter in eqs 2 and 6 is simply $\chi = \chi_{TS} = 0$. Figure 2A shows the adsorption isotherms (φ_C^{surf} as a function of φ_C^{bulk}) for these AOM-type cosolutes of different sizes. The corresponding changes in free energy are shown in Figure 2B as a function of the osmotic pressure. For cosolute and solvent with equal molecular size, the volume fraction of cosolute in the bulk and surface domains is equal, $\varphi_S^{surf} = \varphi_C^{bulk}$, and hence $\Delta\Delta F = 0$ at all cosolute concentrations. For larger cosolutes, size exclusion from the

DOI: 10.1021/acs.jctc.5b00258
J. Chem. Theory Comput. 2015, 11, 3478−3490

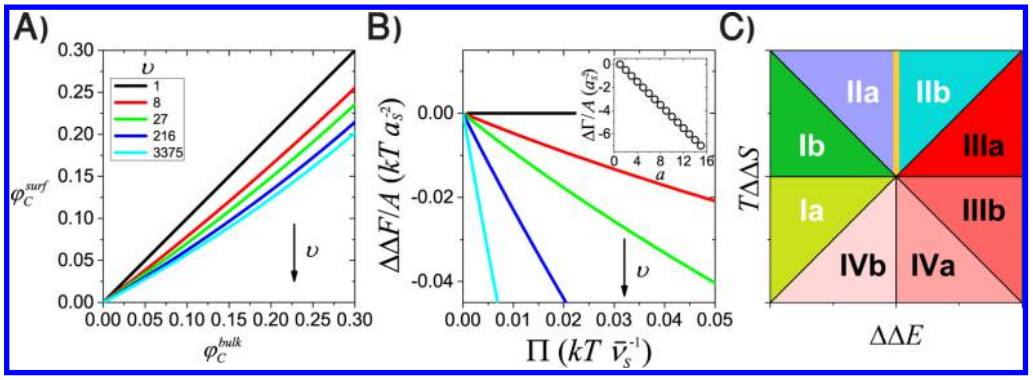

Figure 2. MFC in the Asakura−Oosawa limit. **A)** Adsorption isotherms for cosolutes of different sizes showing stronger exclusion with increasing cosolute size. **B)** The change in association free energy, $\Delta\Delta F/A$, varies linearly with osmotic pressure. Colors as in panel A. **Inset:** The preferential interaction coefficient scales as cosolute linear dimension, a. **C)** Schematic of an entropy-energy plot, delineating eight possible cosolute thermodynamic mechanisms (see text). The sector labels in white and black correspond to stabilizing and destabilizing cosolutes, respectively. All AOM cosolutes reside on the orange line.

surface results in a lowering of the free energy with surface burial, indicating added stabilization of interface association or burial. The cosolutes form an exclusion layer near the surface, whose volume grows linearly with a, eq 1, so that the preferential hydration coefficient also varies linearly with a, Figure 2B inset. Thus, in this AOM limit, the entire cosolute-induced effect directly results from the extent of cosolute exclusion from the surface domain, which depends on cosolute size through a.

To describe the balance between the entropic and energetic contributions to the stabilization free energy, it is convenient to use entropy-energy plots, Figure 2C. The full compensation diagonal, $\Delta\Delta E = T\Delta\Delta S$, separates stabilizing and destabilizing cosolutes (as labeled in the figure by white and black fonts, respectively). The other diagonal $\Delta\Delta E = -T\Delta\Delta S$, separates cosolutes that exert energetically dominated effects from entropically dominated ones. The two diagonals, along with the two main axes, dissect the plot into eight sectors, each corresponding to a different thermodynamic mechanism. Notably, since AOM cosolutes act through a purely entropic mechanism, data from such cosolutes would all reside along the line for which $\Delta\Delta E = 0$. Indeed, this is the MFC result when we set $\chi = \chi_{TS} = 0$ and $\varepsilon = \varepsilon_{TS} = 0$, as shown by the orange line in Figure 2C. In contrast, osmolytes were found experimentally to induce energetic depletion forces while decreasing the entropy, limiting the corresponding data to reside in domain Ia. Finally, some polymeric crowders, which induce entropically dominated depletion forces, typically lead to data points that reside in sectors IIA and IIb. In the next sections we show how all these cosolute classes can be fully accounted for by MFC simply by varying the energetic parameters away from the AOM (i.e., zero energy) values.

3.2. The Ideal Solution Limit. For an ideal cosolute-solvent solution lacking nonideal mixing terms, $\chi = \chi_{TS} = 0$, the only remaining relevant parameters are the cosolute size υ and the parameters quantifying the cosolute interaction with the interface, ε and ε_{TS}. We first consider the case where in addition $\varepsilon_{TS} = 0$, implying that the short-range interaction with the macromolecular surface is purely energetic.

For each cosolute, defined by its values of υ and ε, we assign one of the thermodynamic sectors labeled in the entropy-energy plot, Figure 2C, according to the values of $\Delta\Delta E$ and $T\Delta\Delta S$ in the limit $\varphi_C^{bulk} \to 0$. The resulting sectorgram, Figure 3A, delineates the possible thermodynamic sectors for the different cosolutes that are separated by loci defined by the same conditions separating the sectors in Figure 2C. Similar sectorgrams could be constructed for other values of φ_C^{bulk}; however, this does not change the subsequent qualitative discussions. The balance between entropy and energy in the microscopic cosolute-surface interaction is thus reflected in (and maps onto) the macroscopic energetic and entropic components of the subsequent depletion interaction, as witnessed in the sectorgram.

We find that the AOM limit is only exactly realized for $\varepsilon = 0$ (orange line in Figure 3A), whereas for any $\varepsilon \neq 0$ the depletion force has an additional energetic component. Hence, cosolutes with $\varepsilon_{TS} = 0$ can either exert energetic destabilization (sector IIIa) or alternatively induce stabilization (sectors Ib and II), Figure 3A. Interestingly, below a certain size, the cosolute can act by an energetically dominated mechanism, $\Delta\Delta E < -T\Delta\Delta S$ (sector Ib).

We have recently shown analytically,[11,43] that a similar sectorgram emerges when we consider a simple effective potential of mean force between surface and cosolute. Specifically, in addition to the hard repulsion core (as in AOM), this coarse-grained potential of mean force has an interacting layer representing longer-ranged "soft" cosolute-interface effective repulsion. In the MFC model, the hard-core repulsion is accounted for by eq 5, and ε determines the properties of the additional interacting layer, which can be either repulsive, $\varepsilon > 0$, or attractive, $\varepsilon < 0$. Interestingly, for an ideal solution, the more detailed MFC that incorporates the solvent explicitly converges to give the same qualitative results as the coarser-grained model. In both models, when the AOM hard-core interaction is augmented by an additional energetic interaction (either repulsive or attractive) the thermodynamic mechanism is no longer fully entropic.

The deviation from the AOM prediction is also evident in the extent of stabilization or destabilization that directly impacts the magnitude of $\Delta\Gamma$. While AOM and the macromolecular crowding theory ascribe the cosolute effects to steric interactions, Figure 3B shows that not only does $\Delta\Gamma$ need not correspond to the cosolute size, υ but that it can also depend sensitively on ε. Although $\Delta\Gamma$ is linear in a for AOM-type cosolutes ($\varepsilon = 0$) as well as for cosolutes with $\varepsilon \neq 0$ (Figure 3B, inset), the free energy slope for both with cosolute concentration is much different. Taken together, we conclude that $\Delta\Gamma$ is influenced by, but is not equal to, the molecular

DOI: 10.1021/acs.jctc.5b00258
J. Chem. Theory Comput. 2015, 11, 3478−3490

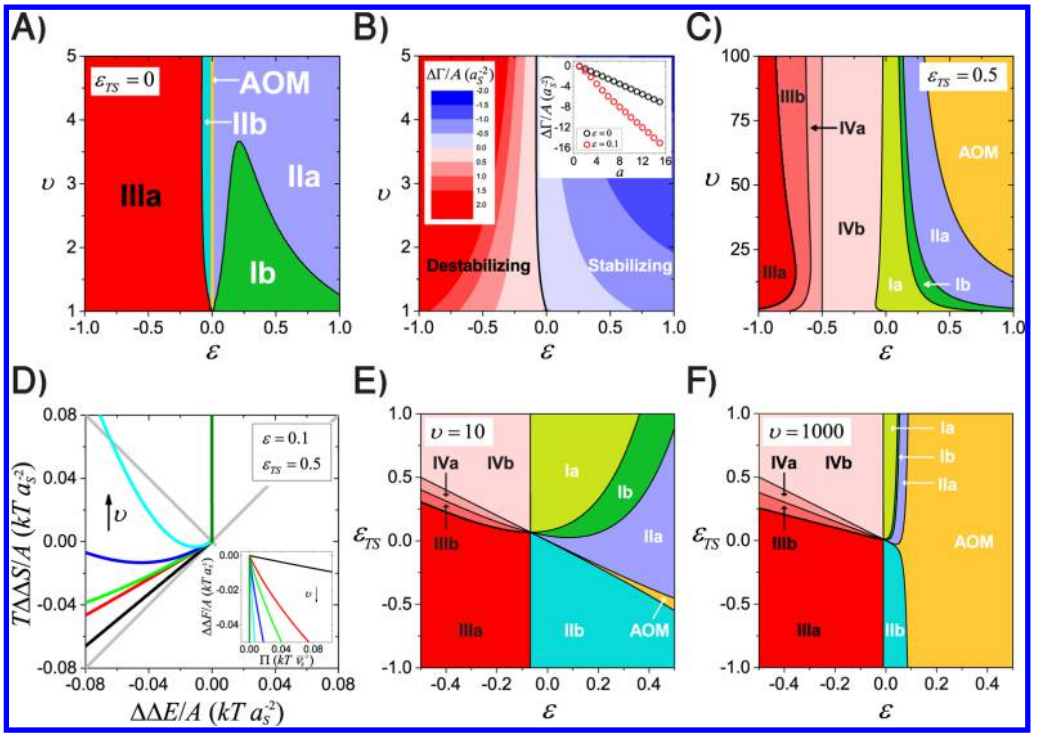

Figure 3. Cosolute impact in ideal solutions. **A)** The ε,υ sectorgram for an ideal solution, $\chi = \chi_{TS} = 0$, with no entropic contribution to the surface interaction ε (i.e., $\varepsilon_{TS} = 0$). **B)** The magnitude of $\Delta\Gamma/A$, represented by color, for the same ε,υ plane as in (A). **Inset:** The preferential interaction coefficient for cosolutes of $\varepsilon = 0.1$ (blue) compared to AOM cosolutes (black). **C)** The ε,υ sectorgram for an ideal solution with an entropic component to the surface interaction, $\varepsilon_{TS} = 0.5$. **D)** The entropy-energy plot for cosolutes of different sizes with $\varepsilon = 0.1$ and $\varepsilon_{TS} = 0.5$. Each line corresponds to the locus formed by different concentrations. **Inset:** The change in free energy for these cosolutes as a function of osmotic pressure. Colors correspond to different cosolute size: $\upsilon = 1$ (black), 8 (red), 27 (light green), 216 (blue), 3375 (cyan), and $\upsilon \to \infty$ (dark green). **E)** The $\varepsilon,\varepsilon_{TS}$ sectorgram for an ideal solution, $\chi = \chi_{TS} = 0$, for cosolute of size $\upsilon = 10$. **F)** The same sectorgram as in (E) only with $\upsilon = 1000$. For all sectorgrams (A, C, E, and F), the available cosolute parameters are specified on each panel, and colors and numbers are as in Figure 2C. The sectorgrams show the same loci (black lines) as in Figure 2C. The orange line corresponds to the AOM cosolutes (with a curve that deviates only slightly, ±1 degree, from the vertical in the entropy-energy plane, Figure 2C).

excluded volume. Thus, one can only speak of an "effective" excluded volume, proportional to $\Delta\Gamma$, that is determined not only by cosolute molecular size but also by its interactions. It is, therefore, insufficient to consider molecular volumes alone when predicting cosolute action.

Let us next consider ε that is temperature-dependent, thereby adding a nonzero entropic component, ε_{TS}. Whereas fixing ε while varying ε_{TS} leaves $\Delta\Gamma$ unaffected, this variation does change the balance between the energetic and entropic components of $\Delta\Delta F$. Setting $\varepsilon_{TS} = 0.5$, for example, changes the ε,υ sectorgram dramatically (compare $\varepsilon_{TS} = 0.5$, Figure 3C to the case of $\varepsilon_{TS} = 0$, Figure 3A) allowing access to all thermodynamic sectors, including those for which $T\Delta\Delta S < 0$. Moreover, these energetically driven regions in the sectorgram persist even for much larger cosolute sizes, υ (higher ordinate values in Figure 3C), making it possible also for large cosolutes to exert energetic depletion forces.

Figure 3D shows the change in the cosolute effect with increasing size as manifested in the entropy-energy plane. As a representative case, we set $\varepsilon = 0.1$ and $\varepsilon_{TS} = 0.5$. These parameters correspond to overall repulsive cosolute interactions with the interface. This repulsion, in turn, is the sum of a microscopic *energetic repulsion* contribution that outweighs a slightly smaller *entropic attraction*. For small-sized cosolutes, the net effect on $\Delta\Delta F$ is energetically dominated, sectors Ia and Ib. As cosolute size increases, the underlying thermodynamic mechanism of the depletion attraction gains a considerable entropic contribution. As a result, for larger cosolutes the mechanism shifts to the entropically dominated sector (II), so that in the limit of very large cosolutes the mechanism converges to the AOM mechanism.

The entropy-energy interplay for cosolutes of different size in an ideal solution can also be followed in the $\varepsilon,\varepsilon_{TS}$ sectorgram, Figure 3E,F. Comparing these two panels, we find that for the larger cosolute, $\upsilon = 1000$ (Figure 3F), the area in the appropriate sectorgram that corresponds to the AOM (excluded-volume-only) locus extends over a larger part of parameter space compared to $\upsilon = 10$ (orange areas in Figures 3F,E). This difference reflects that larger cosolutes are less sensitive to changes in the short-ranged cosolute-interface interaction parameters, which in turn simply reflects the relatively smaller part of these cosolutes that can come in contact with the interface.

Taken together, in an ideal solution the depletion force can be energetically dominated for certain values of υ and ε, even when the microscopic cosolute-interface interaction is completely energetic ($\varepsilon_{TS} = 0$), Figure 3A. However, to induce energetic depletion forces that come with *a net decrease in entropy* (sector Ia), the cosolute-interface interaction must also be temperature dependent, Figure 3C. We have recently shown that the same conclusion can be reached by replacing ε with a potential of mean force that is an effective function of the solvent, cosolute, and interfacial interactions.[11]

DOI: 10.1021/acs.jctc.5b00258
J. Chem. Theory Comput. 2015, 11, 3478−3490

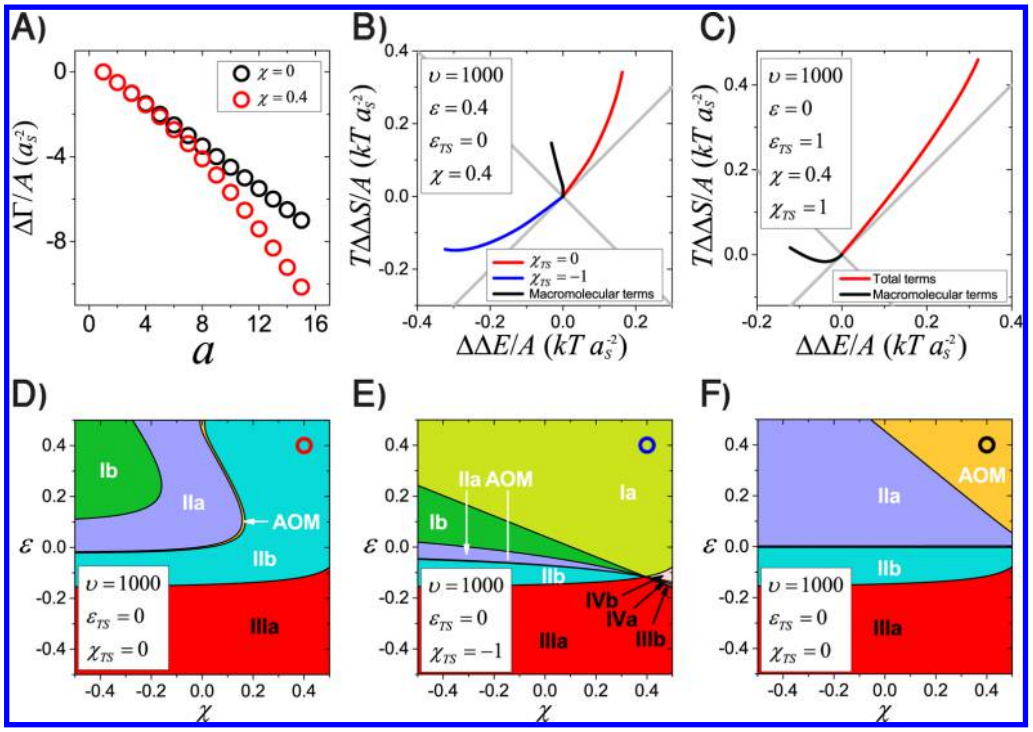

Figure 4. Cosolute effects in nonideal solutions. **A**) The preferential interaction, $\Delta\Gamma/A$, for cosolutes forming a regular solution with $\chi = 0.4$ and $\varepsilon = \varepsilon_{TS} = \chi_{TS} = 0$ (red) compared to AOM cosolutes, where also $\chi = 0$ (black). **B**) Entropy-energy plots for the total and macromolecular (surface) terms of the cosolutes parameters marked by the open circles in (D), (E), and (F). **C**) The entropy-energy plot for the total and macromolecular terms of cosolute with $\upsilon = 1000$, $\varepsilon = 0$, $\varepsilon_{TS} = 1$, $\chi = 0.4$, and $\chi_{TS} = 1$. **D**) The ε,χ sectorgram for a cosolute of size $\upsilon = 1000$ with $\chi_{TS} = \varepsilon_{TS} = 0$. **E**) The same plane as (D) but setting $\chi_{TS} = -1$. **F**) The same sectorgram as (D), but here the colors correspond to the cosolute behavior with respect to only its surface thermodynamic contributions, $\Delta\Delta E_{surf}$ and $T\Delta\Delta S_{surf}$, see text. In panels (D), (E), and (F) the thermodynamic sectors were assigned based on the thermodynamic mechanism at $\varphi_C^{bulk} \approx 0.04$.

3.3. Nonideal Solutions. We turn to consider nonideal solutions, for which $\chi \neq 0$. This adds a free energy component to the mixing of cosolute and solvent in addition to the ideal entropy of mixing in the binary solvent-cosolute mixture, eqs 2 and 6. We start by discussing the regular solution limit,[67] for which χ is purely energetic, so that $\chi_{TS} = 0$ (and for simplicity also set $\varepsilon_{TS} = 0$). For a positive mixing parameter $\chi > 0$, corresponding to disfavored mixing in the bulk domain, the cosolute stabilization effect increases, Figure 4A. However, in comparison to the ideal solution, Figure 3A, the introduction of a nonzero mixing parameter, χ, does not change the thermodynamic features of cosolutes in the ε,υ sectorgram as long as the cosolute is small, Figure S1A in the Supporting Information (SI). Again, as for ideal solutions, setting $\varepsilon_{TS} = 0.5$ allows various thermodynamic sectors to become available (Figure S1B in the SI). In contrast, for a large cosolute size, $\upsilon = 1000$ (with $\varepsilon_{TS} = \chi_{TS} = 0$), the χ,ε sectorgram in Figure 4D demonstrates that only the entropically favored sectors, $T\Delta\Delta S/A > 0$, are accessible.

Allowing a free energy mixing parameter with a nonzero entropic component, $\chi_{TS} \neq 0$, strongly impacts the thermodynamic mechanism. For example, the stabilizing sector Ia (for which $T\Delta\Delta S < 0$) becomes accessible simply by setting $\chi_{TS} = -1$, so that the microscopic cosolute-solvent interaction is entropically disfavored, as shown in the ε,υ plane (Figure S1A,C in the SI). The same effect is seen in the dramatic change of the ε,χ sectorgram, Figure 4E. In fact, even in the absence of direct cosolute-interface interaction ($\varepsilon = \varepsilon_{TS} = 0$), we find that there are considerable energetic contributions to the depletion force, Figure 4D,E. Specifically, we find that cosolutes may incur either an energetic penalty (Figure 4D) or an energetic gain (Figure 4E) in the depletion attraction.

3.4. Entropy-Enthalpy Compensation in Nonideal Solutions and the Role of Macromolecular versus Solution Terms. It has been previously appreciated that the underlying thermodynamic mechanism of cosolute-induced stabilization (or destabilization) can often be obscured by entropic and enthalpic contributions resulting from the solvent, which do not, however, directly affect $\Delta\Delta F$.[12−15] Specifically, the total (or "experimentally apparent") thermodynamic components, $\Delta\Delta E$ and $T\Delta\Delta S$, can each be dissected into two terms: one that includes all contributions from the surface (macromolecular) interactions (both with solvent and cosolute) and the other that includes all other interactions (solvent-solvent, cosolute-cosolute, and solvent-cosolute). Hence, for the incompressible lattice system, the free energy can be written as

$$\Delta\Delta F = \Delta\Delta E_{surf} + \Delta\Delta E_{solution} - T(\Delta\Delta S_{surf} + \Delta\Delta S_{solution}) \quad (12)$$

It was further shown that the solution components exactly cancel out, $\Delta\Delta E_{solution} = T\Delta\Delta S_{solution}$, so that the free energy change is only directly determined by the surface (or macromolecular) terms:

$$\Delta\Delta F = \Delta\Delta E_{surf} - T\Delta\Delta S_{surf} \quad (13)$$

It is important to note that the solution components still *implicitly* affect the free energy change through their influence on the equilibrium state. However, since only the surface terms directly alter $\Delta\Delta F$, it is instructive to examine them separately.

DOI: 10.1021/acs.jctc.5b00258
J. Chem. Theory Comput. 2015, 11, 3478−3490

Indeed, we have recently shown that taking only the surface-cosolute interaction into account in a simple analytical model suffices to reproduce most of the possible cosolute-induced mechanisms.[11,43]

The dissection into solution and macromolecular related terms is also important because the AOM interpretation is related to (and in fact considers from the outset) only the macromolecular terms, because it treats the solvent only implicitly and neglects its energetic and entropic components. It is therefore illuminating to determine the state of the same macromolecular terms wherever there is a net energetic contribution to the free energy. It should be emphasized that while $\Delta\Delta F$, $\Delta\Delta E$, and $T\Delta\Delta S$ can be accessed experimentally by various methods,[31] there is no current method to measure specifically the surface related terms, $\Delta\Delta E_{surf}$ and $T\Delta\Delta S_{surf}$. In simulations and analytic models, however, one can directly quantify these terms.[15,43] In the following, we dissect these surface and solution contributions to further expose the underlying thermodynamic mechanisms.

Focus first on cosolutes described in Figure 4D and 4E, for which the interface-cosolute interaction parameters are the same. With respect to their surface-related terms, eq 13, the two cosolutes share the same ε,χ sectorgram, Figure 4F. Strikingly, Figure 4F is very different from both Figure 4D and E. Perhaps most interestingly, the total entropic and energetic contributions for a cosolute can *appear* to act according to one thermodynamic mechanism, while the relevant, surface related terms that directly contribute to the free energy changes indicate *a different* mechanism.

For example, the cosolute indicated by the red open circle in Figure 4D appears to act by an entropically dominated mechanism with energetic mitigation (sector IIb). However, the surface terms for the same cosolute in Figure 4F (black open circle) indicate that the underlying mechanism is fully entropic and in line with the AOM. Changing a single solution parameter, so that $\chi_{TS} = -1$, does not alter the surface related terms (fully entropic, black open circle in Figure 4F) but causes the cosolute to *appear* to act by an energetically driven mechanism (with entropic mitigation), blue open circle in Figure 4E. The difference between the surface and total components can be conveniently shown in the entropy-energy plot, Figure 4B (line colors correspond to colored open circles in Figure 4D, E, and F). Interestingly, the depletion force can also *appear* to act entropically (sector IIb), while the macromolecular terms reveal the underlying mechanism is energetically driven and entropically disfavored (sector Ia), Figure 4C.

These examples demonstrate that the apparent thermodynamic mechanism, as determined by $\Delta\Delta E$ and $T\Delta\Delta S$, can reflect or completely contradict the underlying thermodynamic mechanism inferred by the surface related terms, $\Delta\Delta E_{surf}$ and $T\Delta\Delta S_{surf}$, which are the only ones that directly contribute to $\Delta\Delta F$. This incongruence poses an experimental challenge for resolving the molecular mechanism of cosolute action on macromolecules. While the underlying molecular mechanism is more directly related to the surface related terms, current experimental methods are mostly designed to access the total entropic and energetic components.

3.5. Comparing Theory with Protein Folding Experiments. Having demonstrated in the previous sections the wide range of cosolute mechanisms that can lead to macromolecular stabilization, we turn now to compare the theoretical predictions with available experiments of the cosolute stabilizing effect. While the MFC is not designed to provide quantitative fits to experiments, the aim of this comparison is rather to establish general links between the microscopic model parameters and the macroscopically measured cosolute-induced effects on proteins, as they are seen in experiments.

Accumulating experimental evidence suggest that most (neutral) cosolutes, and specifically those that are naturally occurring, belong to one of three "families", each with its unique thermodynamic mechanism of impacting macromolecular processes such as protein folding.[11,30,31] Protective osmolytes exert energetically dominated stabilization and decrease the macromolecular association entropy,[25,30,31] hence residing in sector Ia, Figure 2C. Polymeric crowders usually exert depletion forces dominated by favorable entropy, with additional, usually small, energetic contributions (sectors IIa and IIb). Notably, even polymeric crowders can sometimes exert energetically dominated depletion forces.[34] The third group consists of chemical denaturants, of which urea is a prime example. In the following we demonstrate how MFC can account for the effect of cosolutes from all three families.

The model parameters that describe cosolutes in solution (υ, χ, and χ_{TS}) have been derived and reported from experiments of binary water-cosolute mixtures (in the absence of proteins or other macromolecules). The cosolute size υ is accessible through cosolute molar volumes. The mixing parameter, χ, can be estimated through fitting of experimental osmotic pressure or water activity measurements with the MFC expression for the osmotic pressure, eq 10. The entropic component, χ_{TS}, can also be estimated by fitting the temperature dependence of χ. The parameters derived in this way for several selected cosolutes from the three families, along with details regarding the fitting procedure, are given in Table S1 of the SI. Interestingly, for all stabilizing cosolutes we find $\chi_{TS} < 0$, implying that there is generally an entropic penalty in the nonideal mixing component of these cosolutes with water.

Once the cosolute-solvent parameters have been derived, the model parameters related to cosolute-interface interactions (ε and ε_{TS}) for a particular macromolecular process can then be determined for a given set of derived υ, χ, and χ_{TS}. Since ε_{TS} does not affect the free energy change, $\Delta\Delta F$, the parameter ε can be readily obtained as a fitting parameter for the variation of $\Delta\Delta F$ with osmotic pressure, that in turn determines $\Delta\Gamma$. For comparison of results involving different proteins and different experiments, in this fitting procedure, we normalized the experimental thermodynamic quantities to the change in accessible surface area upon folding, which we calculated using the ProtSa server[68,69] and the relevant pdb files.[70−73] Finally, ε_{TS} can be evaluated from a fit to the experimental entropy-energy dependence of the cosolute.

Figure 5A shows, on entropy-enthalpy plots, the fits to the experimentally derived stabilization effects induced by protective osmolytes for several protein folding processes. Experimentally reported enthalpic changes are directly comparable to the model's energy changes, because of the model lattice incompressibility. For the shown osmolytes, the energetically dominated depletion forces best match values of $\varepsilon \approx 0$ and $\varepsilon_{TS} > 0$, suggesting that the interaction of cosolute with the molecular surface comes at an entropic gain and an energetic penalty.

Once the energetic parameters are set, an important model prediction regards the temperature dependence of $\Delta\Delta F$. Specifically, given the entropic contributions for the interaction parameters, ε_{TS} and χ_{TS}, we can estimate how the stabilization

DOI: 10.1021/acs.jctc.5b00258
J. Chem. Theory Comput. 2015, 11, 3478−3490

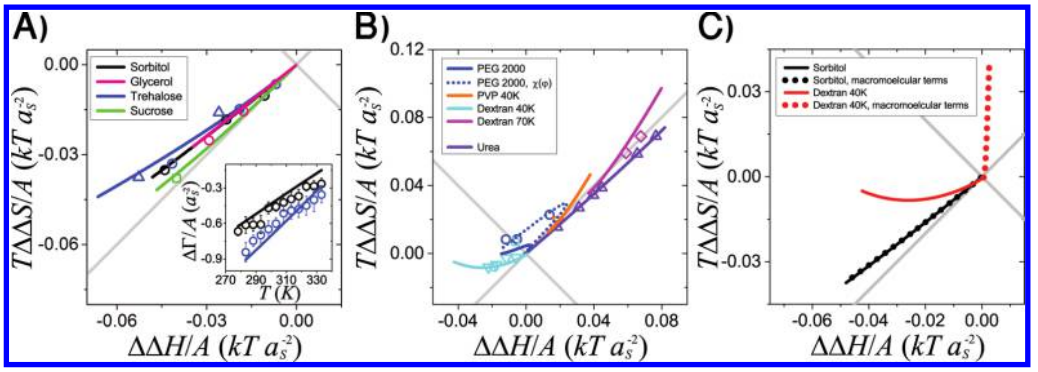

Figure 5. Comparison of the mean field model (lines) with protein folding experiments (empty symbols): the entropy-enthalpy plots of the stabilization induced by different cosolute families. Colors represent different cosolutes, and the symbol shapes represent different proteins: β-hairpin peptide[25,30] (○), α-chymotrypsin[95] (△), chymotrypsin inhibitor 2[29] (□), Ubiquitin[28,34] (▽), and α-lactalbumin[96] (◊). **A)** Protective osmolytes act energetically. **Inset:** The change in $\Delta\Gamma/A$ with temperature in experiment vs the MFC prediction. **B)** Macromolecular crowders can either act entropically or energetically. The denaturant urea acts energetically. The data for PVP 40K is at T = 340 K. The dotted blue line represents fits based on concentration dependence for χ. **C)** The apparent thermodynamic breakdown into $\Delta\Delta H$ and $T\Delta\Delta S$ alongside the macromolecular (surface) terms, $\Delta\Delta H_{surf}$ and $T\Delta\Delta S_{surf}$, for Dextran 40K and sorbitol. In all panels, since the lattice model is incompressible, we directly compare energy changes predicted by the model with the experimentally derived enthalpic values. In comparing the experimental values to the model, we used $a_S = \sqrt[3]{30}$ Å. All other parameters used in these fits are available in the SI.

effect varies with temperature. For sorbitol and trehalose, for example, the model predicts that the preferential interaction, $\Delta\Gamma/A$, will increase with increasing temperature. This prediction shows a very good quantitative fit to experiments, Figure 5A, inset.

Polymeric crowders show more diverse properties in the entropy-enthalpy plane, that include either enthalpically or entropically dominated impacts, depending on the cosolute and details of the macromolecular process, Figure 5B. Echoing this variability, the MFC parameters for these cosolutes are more varied, too. For example, for dextran 40KD, used in the experiments whose results are reproduced in Figure 5B, we determine $\varepsilon < 0$ and $\varepsilon_{TS} > 0$, resulting in favorable energetic contribution to the depletion effect. However, for dextran 70KD, used in other experiments, we determine $\varepsilon_{TS} < 0$, which results in entropically favorable depletion force. This variability also reflects the fact that for these large cosolutes, the MFC fit is far less sensitive to the value of ε_{TS} than it is for smaller cosolutes.

For PEG2000, the cosolute-induced stabilization mechanism shifts between thermodynamic sectors as a function of concentration, Figure 5B. The current model can account for this shift qualitatively (solid blue curve). Yet, a much better fit (dotted blue line) results when we also account for the concentration dependence of the interaction parameter and its entropic and enthalpic components, by defining

$$\chi(\phi_C) = \chi^0 + \chi^\phi \phi_C$$
$$\chi_{TS}(\phi_C) = \chi_{TS}^0 + \chi_{TS}^\phi \phi_C \quad (14)$$

Such concentration dependence of the FH parameters have been previously reported and measured experimentally.[74−77] This indicates that the limited set of fundamental parameters used in regular solution theory may be insufficient when the solution mixing properties change with concentration, which may prove crucial to making more quantitative predictions. Accounting for concentration-dependent interaction parameters is somewhat analogous to considering MFC parameters that are different in the bulk and the surface domain, thereby establishing different mixing properties in the two domains.

Urea, as a chemical denaturant that resides in sector IIIa (Figure 5B), induces destabilization that is driven by enthalpy, with an entropic component that is stabilizing. However, controversy still persists regarding the molecular mechanism that leads to these entropic and energetic contributions.[15,59,78−80] In the context of MFC, the cosolute shows attractive free energy contributions ($\varepsilon < 0$), and in contrast to protective osmolytes, the MFC model is able to reproduce the experimental results by assigning an entropy loss upon cosolute-surface interaction, $\varepsilon_{TS} < 0$. Unlike for stabilizers, the urea experimental data could be well fit only if we allow $f < 1$, which is consistent with the number of nearest neighbors diminishing at the surface domain. This may come as no surprise, since urea adsorbs to the surface, making the model more sensitive to the different mixing parameters at the surface. This also underscores the possible differences in the solution mixing parameters, χ and χ_{TS}, between bulk and surface that is reflected within MFC as changes in f. We note, however, that MFC is unable to account for correlated interactions, including surface-to-surface "bridging interactions" which have recently been suggested to play a role in urea's action and in cosolute-induced polymer collapse.[81,82] To incorporate such interactions it would be necessary to extend the theory beyond simple mean field so as to explicitly account for possible correlations between solution components.[81,82]

By returning to the delineation into solution and macromolecular components, as described in section 3.4, we can gain further insight into the underlying mechanism invoked by different cosolutes, Figure 5C. Strikingly, although for dextran 40K the cosolute effect *appears* energetic, the macromolecular terms reveal an underlying entropic affect. This allows to reconcile AOM with the action of many polymeric crowders; although they may appear to act energetically, thereby contradicting the AOM predictions, their macromolecular terms can still conform to the AOM. To contrast, the osmolyte sorbitol appears to act energetically, as also supported by the macromolecular terms. This indicates that the AOM is probably fundamentally inapplicable to sorbitol, even when only the macromolecular terms are considered. This discrepancy suggests that sorbitol and similar osmolytes act through a separate mechanism that is distinct from polymeric crowders,

DOI: 10.1021/acs.jctc.5b00258
J. Chem. Theory Comput. 2015, 11, 3478−3490

whereby the dominating contribution originates from the temperature dependence of cosolute-macromolecular interface interactions.

4. SUMMARY AND CONCLUSIONS

We have proposed a mean field model based on regular solution theory (MFC) to explain the full gamut of cosolute effects on macromolecules. In addition to excluded volume effects related to cosolute size, we included two important components: an interaction between chemical species in the bulk and a short-ranged interaction between cosolute and the interface/macromolecule (adsorption-like term). Moreover, we regard these microscopic interactions as effective free-energies with entropic and energetic parts.

Despite its relative simplicity, this model can capture many features of diverse cosolute families. Specifically, within MFC, the combination of solution mixing and cosolute-interface interaction parameters can result in a depletion force that is energetically favorable and entropically *disfavored*, sector Ia in Figure 2C. This, perhaps nonintuitive result, has been shown experimentally for protective osmolytes as well as for some polymeric crowders. The same formalism can also account for energetically mitigated depletion forces, sector IIa, and even for chemical denaturants, sector IIIa. The diversity in thermodynamic "fingerprints" naturally emerges by explicitly accounting for intermolecular interaction in the mean field limit between all solution components.

For osmolyte cosolutes, MFC further allows us to trace the energetically driven depletion forces with entropic penalty (sector Ia) to effective microscopic cosolute-interface interactions that are concertedly *energetically repulsive* and *entropically attractive*. This prediction is in complete agreement with our recent coarse grained model based on the Kirkwood-Buff solution theory and by considering simple potentials of mean force between cosolute and macromolecule.[11] This also agrees with molecular dynamics simulations of sorbitol, which demonstrate cosolute-induced variations in the entropy associated with the first hydration layer around proteins.[63]

For much larger cosolutes, such as polymers, that are typically referred to as macromolecular crowders, we generally find induced depletion forces with both entropic and energetic contributions. For these cosolutes the entropic components of the depletion force usually dominate, in accordance with the Asakura and Oosawa model (AOM), with only small energetic contributions (sectors IIa and IIb in Figure 2C).

Interestingly, we find that through a combination of mixing and cosolute-macromolecule interaction parameters, it is possible for large macromolecular crowders to induce depletion forces that also incur an *entropic penalty* and hence reside in sector Ia (see, e.g. Figure 4E). This is supported by the experimentally determined values for protein stabilization by dextran.[34] Importantly, for these energetically driven depletion forces, the entropic and energetic contributions, $\Delta\Delta E$ and $T\Delta\Delta S$, are dominated by solution terms that do not directly impact the net stabilization, $\Delta\Delta F$. However, contributions of the cosolute-interface terms, $\Delta\Delta E_{surf}$ and $T\Delta\Delta S_{surf}$, which are the ones that directly impact $\Delta\Delta F$, indicate a mechanism reminiscent of AOM. We conclude that this AOM-like depletion force that is most relevant for polymers is merely obscured by changes in the solution energy and entropy, $\Delta\Delta E_{solution}$ and $T\Delta\Delta S_{solution}$, so that in total the entropic and energetic contributions *appear* to reside in sector Ia. This trend also agrees with our results from Monte Carlo simulations of simple molecular mixtures.[43]

Taken together, we conclude that energetically driven depletion forces that are also entropically disfavored (sector Ia, Figure 2C) can have two completely *different* molecular mechanisms. For protective osmolytes these forces originate from effective cosolute-macromolecule interactions that are entropically attractive and energetically repulsive. In contrast, for polymeric crowders they may only *appear* energetically driven, due to the overwhelming entropic and energetic contributions from solution interactions. The underlying macromolecular terms of these polymeric crowders, however, reveal an entropic mechanism that essentially fits the mechanism proposed by Asakura and Oosawa.

The entropy-energy balance of cosolute-induced protein stabilization determined here and in previous studies serves as a constraint in the quest for identifying plausible underlying mechanisms. In order to verify the predictions presented here regarding protein folding processes, it would be necessary to directly investigate the temperature-dependence of solution parameters. Specifically, the cosolute-surface interactions, often studied in terms of "transfer free energies",[54−57,59,60] could, in principle, be further dissected into entropic and energetic terms[15] (that in MFC are manifested in ε and ε_{TS}). This can be achieved, for example, by determining the temperature dependence of the relevant transfer free energies. This would, in turn, allow better predictions of the transfer model that would accurately account not only for the cosolute-induced effects but also for their temperature dependence.

Our predictions could also gain support from measurements of the cosolute-solvent interactions (with and without the interface/macromolecule). The molecular properties of osmolyte aqueous solutions have been studied extensively.[83−88] For example, osmolytes are known to modify the hydrogen bond properties in solution,[86,89−92] so that different concentrations of cosolute in the surface and bulk domains should change the entropy-energy balance. The interaction free energy parameters, ε and χ, and their entropic components, ε_{TS} and χ_{TS}, are necessarily related to these hydration properties. Additional thermodynamic analysis of solution restructuring around macromolecules can shed light on the molecular origins of these empirical parameters.

Furthermore, it would be worthwhile to dissect the energetic and entropic changes associated with cosolute-induced effects and link them with their respective macromolecular and solution terms. Currently, while this subdivision is accessible in theory and simulations, it has not been determined experimentally. Since the solution terms are typically large and therefore can obscure the underlying molecular mechanism, theoretical models and simulations are required to determine the size of these contributions. Future experiments that are surface sensitive may be able to resolve these interactions.

The cosolute-induced shift in protein folding equilibria, or more generally of macromolecular compaction, is often described at the mean field level in terms of polymer transfer to solvents of different quality.[27,93,94] Our approach focuses on the entropic and enthalpic components of the molecular-level solution interactions and thus allows for accounting for the temperature dependence of the cosolute effect. However, our mean field theory does not account for correlations between molecules. Thus, in its current form, this theory is not well suited to describe effects that involve the concerted

DOI: 10.1021/acs.jctc.5b00258
J. Chem. Theory Comput. 2015, 11, 3478−3490

organization of cosolutes and macromolecules, as for example in the case of "bridging interactions".[81,82]

To conclude, accumulating evidence from a variety of experimental methods suggests that excluded cosolutes that induce depletion forces act through thermodynamically distinct mechanisms. Specifically, macromolecular crowders and protective osmolyte differ in the temperature dependence of their stabilization effect. Theoretical models are helpful in resolving the molecular mechanisms that lead to these apparent differences. It is intriguing to speculate whether the same mechanistic differences have also been exploited by different organisms as a means of adaptation to temperature stresses in the perpetual struggle to preserve protein integrity.

■ ASSOCIATED CONTENT

Supporting Information

The effect of the solution mixing parameter on the depletion force in the ε,υ sectorgram, as well as a table with the experimentally determined parameters of the model. The Supporting Information is available free of charge on the ACS Publications website at DOI: 10.1021/acs.jctc.5b00258.

■ AUTHOR INFORMATION

Corresponding Author

*E-mail: daniel.harries@mail.huji.ac.il.

Author Contributions

The manuscript was written through contributions of all authors. All authors have given approval to the final version of the manuscript.

Notes

The authors declare no competing financial interest.

■ ACKNOWLEDGMENTS

The financial support from the Israel Science Foundation (ISF grant No. 1538/13) is gratefully acknowledged. L.S. is supported by the Adams Fellowship Program of the Israel Academy of Sciences and Humanities. The Fritz Haber Research Center is supported by the Minerva Foundation, Munich, Germany.

■ REFERENCES

(1) Parsegian, V. A. Protein-Water Interactions. *Int. Rev. Cytol.* **2002**, *215*, 1−31.

(2) Lekkerkerker, H. N. W.; Tuinier, R. *Colloids and the Depletion Interaction*; Springer: Heidelberg, Germany, 2011.

(3) Hochachka, P. W.; Somero, G. N. *Biochemical Adaptation*; Oxford University Press: New York, NY, 2002; pp 217−289.

(4) Yancey, P. H.; Clark, M. E.; Hand, S. C.; Bowlus, R. D.; Somero, G. N. Living with Water-Stress - Evolution of Osmolyte Systems. *Science* **1982**, *217*, 1214−1222.

(5) Yancey, P. H. Organic Osmolytes as Compatible, Metabolic and Counteracting Cytoprotectants in High Osmolarity and Other Stresses. *J. Exp. Biol.* **2005**, *208*, 2819−2830.

(6) Lindquist, S. L.; Kelly, J. W. Chemical and Biological Approaches for Adapting Proteostasis to Ameliorate Protein Misfolding and Aggregation Diseases: Progress and Prognosis. *Cold Spring Harbor Perspect. Biol.* **2011**, *3*, a004507.

(7) Gibbs, J. W. On the Equilibrium of Heterogeneous Substances. *Trans. Conn. Acad. Arts Sci.* **1876**, *3*, 108−248/343−524.

(8) Greene, R.; Pace, C. Urea and Guanidine Hydrochloride Denaturation of Ribonuclease, Lysozyme, A-Chymotrypsin, and B-Lactoglobulin. *J. Biol. Chem.* **1974**, *249*, 5388−5393.

(9) Kirkwood, J. G.; Buff, F. P. The Statistical Mechanical Theory of Solutions. I. *J. Chem. Phys.* **1951**, *19*, 774−777.

(10) Shimizu, S.; Matubayasi, N. Preferential Solvation: Dividing Surface vs Excess Numbers. *J. Phys. Chem. B* **2014**, *118*, 3922−3930.

(11) Sapir, L.; Harries, D. Is the Depletion Force Entropic? Molecular Crowding beyond Steric Interactions. *Curr. Opin. Colloid Interface Sci.* **2015**, *20*, 3−10.

(12) Ben-Naim, A. Hydrophobic Interaction and Structural Changes in the Solvent. *Biopolymers* **1975**, *14*, 1337−1355.

(13) Yu, H.-A.; Karplus, M. A Thermodynamic Analysis of Solvation. *J. Chem. Phys.* **1988**, *89*, 2366.

(14) Ben-Naim, A. *Molecular Theory of Water and Aqueous Solutions. Part I: Understanding Water*; World Scientific: Singapore, 2009; pp 311−322.

(15) van der Vegt, N. F. A.; Trzesniak, D.; Kasumaj, B.; van Gunsteren, W. F. Energy-Entropy Compensation in the Transfer of Nonpolar Solutes from Water to Cosolvent/water Mixtures. *ChemPhysChem* **2004**, *5*, 144−147.

(16) Asakura, S.; Oosawa, F. On Interaction between Two Bodies Immersed in a Solution of Macromolecules. *J. Chem. Phys.* **1954**, *22*, 1255−1256.

(17) Asakura, S.; Oosawa, F. Interaction between Particles Suspended in Solutions of Macromolecules. *J. Polym. Sci.* **1958**, *33*, 183−192.

(18) Minton, A. Excluded Volume as a Determinant of Macromolecular Structure and Reactivity. *Biopolymers* **1981**, *20*, 2093−2120.

(19) Cheung, M. S.; Klimov, D.; Thirumalai, D. Molecular Crowding Enhances Native State Stability and Refolding Rates of Globular Proteins. *Proc. Natl. Acad. Sci. U. S. A.* **2005**, *102*, 4753−4758.

(20) Parsegian, V. A.; Rand, R. P.; Rau, D. C. Osmotic Stress, Crowding, Preferential Hydration, and Binding: A Comparison of Perspectives. *Proc. Natl. Acad. Sci. U. S. A.* **2000**, *97*, 3987−3992.

(21) Christiansen, A.; Wittung-Stafshede, P. Synthetic Crowding Agent Dextran Causes Excluded Volume Interactions Exclusively to Tracer Protein Apoazurin. *FEBS Lett.* **2014**, *588*, 811−814.

(22) Minton, A. P. A Molecular Model for the Dependence of the Osmotic Pressure of Bovine Serum Albumin upon Concentration and pH. *Biophys. Chem.* **1995**, *57*, 65−70.

(23) Bechinger, C.; Rudhardt, D.; Leiderer, P.; Roth, R.; Dietrich, S. Understanding Depletion Forces beyond Entropy. *Phys. Rev. Lett.* **1999**, *83*, 3960−3963.

(24) Jiao, M.; Li, H.-T.; Chen, J.; Minton, A. P.; Liang, Y. Attractive Protein-Polymer Interactions Markedly Alter the Effect of Macromolecular Crowding on Protein Association Equilibria. *Biophys. J.* **2010**, *99*, 914−923.

(25) Politi, R.; Harries, D. Enthalpically Driven Peptide Stabilization by Protective Osmolytes. *Chem. Commun.* **2010**, *46*, 6449−6451.

(26) Koutsioubas, A.; Lairez, D.; Combet, S.; Fadda, G. C.; Longeville, S.; Zalczer, G. Crowding Effect on Helix-Coil Transition: Beyond Entropic Stabilization. *J. Chem. Phys.* **2012**, *136*, 215101.

(27) Badasyan, A.; Tonoyan, S.; Giacometti, A.; Podgornik, R.; Parsegian, V. A.; Mamasakhlisov, Y.; Morozov, V. Osmotic Pressure Induced Coupling between Cooperativity and Stability of a Helix-Coil Transition. *Phys. Rev. Lett.* **2012**, *109*, 068101.

(28) Wang, Y.; Sarkar, M.; Smith, A. E.; Krois, A. S.; Pielak, G. J. Macromolecular Crowding and Protein Stability. *J. Am. Chem. Soc.* **2012**, *134*, 16614−16618.

(29) Benton, L. A.; Smith, A. E.; Young, G. B.; Pielak, G. J. Unexpected Effects of Macromolecular Crowding on Protein Stability. *Biochemistry* **2012**, *51*, 9773−9775.

(30) Sukenik, S.; Sapir, L.; Gilman-Politi, R.; Harries, D. Diversity in the Mechanisms of Cosolute Action on Biomolecular Processes. *Faraday Discuss.* **2013**, *160*, 225.

(31) Sukenik, S.; Sapir, L.; Harries, D. Balance of Enthalpy and Entropy in Depletion Forces. *Curr. Opin. Colloid Interface Sci.* **2013**, *18*, 495−501.

(32) Zhou, H.-X. Polymer Crowders and Protein Crowders Act Similarly on Protein Folding Stability. *FEBS Lett.* **2013**, *587*, 394−397.

(33) Sarkar, M.; Li, C.; Pielak, G. J. Soft Interactions and Crowding. *Biophys. Rev.* **2013**, *5*, 187−194.

(34) Senske, M.; Törk, L.; Born, B.; Havenith, M.; Herrmann, C.; Ebbinghaus, S. Protein Stabilization by Macromolecular Crowding

DOI: 10.1021/acs.jctc.5b00258
J. Chem. Theory Comput. 2015, 11, 3478−3490

through Enthalpy rather than Entropy. *J. Am. Chem. Soc.* **2014**, *136*, 9036−9041.
(35) Schellman, J. A. Protein Stability in Mixed Solvents: A Balance of Contact Interaction and Excluded Volume. *Biophys. J.* **2003**, *85*, 108−125.
(36) Kim, Y. C.; Mittal, J. Crowding Induced Entropy-Enthalpy Compensation in Protein Association Equilibria. *Phys. Rev. Lett.* **2013**, *110*, 208102.
(37) Saunders, A. J.; Davis-Searles, P. R.; Allen, D. L.; Pielak, G. J.; Erie, D. A. Osmolyte-Induced Changes in Protein Conformational Equilibria. *Biopolymers* **2000**, *53*, 293−307.
(38) Davis-Searles, P. R.; Saunders, A. J.; Erie, D. A.; Winzor, D. J.; Pielak, G. J. Interpreting the Effects of Small Uncharged Solutes on Protein-Folding Equilibria. *Annu. Rev. Biophys. Biomol. Struct.* **2001**, *30*, 271−306.
(39) Hall, D.; Minton, A. P. Macromolecular Crowding: Qualitative and Semiquantitative Successes, Quantitative Challenges. *Biochim. Biophys. Acta, Proteins Proteomics* **2003**, *1649*, 127−139.
(40) Zhou, H.-X.; Rivas, G.; Minton, A. P. Macromolecular Crowding and Confinement: Biochemical, Biophysical, and Potential Physiological Consequences. *Annu. Rev. Biophys.* **2008**, *37*, 375−397.
(41) Knowles, D. B.; LaCroix, A. S.; Deines, N. F.; Shkel, I.; Record, M. T., Jr.; Record, M. T. Separation of Preferential Interaction and Excluded Volume Effects on DNA Duplex and Hairpin Stability. *Proc. Natl. Acad. Sci. U. S. A.* **2011**, *108*, 12699−12704.
(42) Minton, A. P. Quantitative Assessment of the Relative Contributions of Steric Repulsion and Chemical Interactions to Macromolecular Crowding. *Biopolymers* **2013**, *99*, 239−244.
(43) Sapir, L.; Harries, D. Origin of Enthalpic Depletion Forces. *J. Phys. Chem. Lett.* **2014**, *5*, 1061−1065.
(44) Egorov, S. Effect of Repulsive and Attractive Interactions on Depletion Forces in Colloidal Suspensions: A Density Functional Theory Treatment. *Phys. Rev. E* **2004**, *70*, 1−8.
(45) Louis, A.; Allahyarov, E.; Löwen, H.; Roth, R. Effective Forces in Colloidal Mixtures: From Depletion Attraction to Accumulation Repulsion. *Phys. Rev. E* **2002**, *65*, 061407.
(46) Shendruk, T. N.; Bertrand, M.; Harden, J. L.; Slater, G. W.; de Haan, H. W. Coarse-Grained Molecular Dynamics Simulations of Depletion-Induced Interactions for Soft Matter Systems. *J. Chem. Phys.* **2014**, *141*, 244910.
(47) Rovigatti, L.; Gnan, N.; Parola, A.; Zaccarelli, E. How Soft Repulsion Enhances the Depletion Mechanism. *Soft Matter* **2015**, *11*, 692−700.
(48) Sarkar, M.; Smith, A. E.; Pielak, G. J. Impact of Reconstituted Cytosol on Protein Stability. *Proc. Natl. Acad. Sci. U. S. A.* **2013**, *110*, 19342−19347.
(49) Flory, P. J. Thermodynamics of High Polymer Solutions. *J. Chem. Phys.* **1942**, *10*, 51−61.
(50) Flory, P. J. *Principles of Polymer Chemistry*; Cornell University Press: Ithaca, New York, 1953; pp 495−540.
(51) Huggins, M. L. Thermodynamic Proerties of Solutions of Long-Chain Compounds. *Ann. N.Y. Acad. Sci.* **1942**, *43*, 1−32.
(52) Huggins, M. L. Some Properties of Solutions of Long-Chain Compounds. *J. Phys. Chem.* **1942**, *46*, 151−158.
(53) Hill, T. L. *An Introduction to Statistical Thermodynamics*; Dover Publications, Inc.: New York, NY, 1986; pp 401−410.
(54) Aune, K.; Tanford, C. Thermodynamics of the Denaturation of Lysozyme by Guanidine Hydrochloride. II. Dependence on Denaturant Concentration at 25. *Biochemistry* **1969**, *8*, 4586−4590.
(55) Auton, M.; Bolen, D. W. Predicting the Energetics of Osmolyte-Induced Protein Folding/unfolding. *Proc. Natl. Acad. Sci. U. S. A.* **2005**, *102*, 15065−15068.
(56) Pegram, L. M.; Record, M. T., Jr. Thermodynamic Origin of Hofmeister Ion Effects. *J. Phys. Chem. B* **2008**, *112*, 9428−9436.
(57) Capp, M. W.; Pegram, L. M.; Saecker, R. M.; Kratz, M.; Riccardi, D.; Wendorff, T.; Cannon, J. G.; Record, M. T., Jr. Interactions of the Osmolyte Glycine Betaine with Molecular Surfaces in Water: Thermodynamics, Structural Interpretation, and Prediction of M-Values. *Biochemistry* **2009**, *48*, 10372−10379.
(58) Diehl, R. C.; Guinn, E. J.; Capp, M. W.; Tsodikov, O. V.; Record, M. T. Quantifying Additive Interactions of the Osmolyte Proline with Individual Functional Groups of Proteins: Comparisons with Urea and Glycine Betaine, Interpretation of M-Values. *Biochemistry* **2013**, *52*, 5997−6010.
(59) Moeser, B.; Horinek, D. Unified Description of Urea Denaturation: Backbone and Side Chains Contribute Equally in the Transfer Model. *J. Phys. Chem. B* **2014**, *118*, 107−114.
(60) Moeser, B.; Horinek, D. The Role of the Concentration Scale in the Definition of Transfer Free Energies. *Biophys. Chem.* **2015**, *196*, 68−76.
(61) Shaw, D. J. *Introduction to Colloid and Surface Chemistry*, 4th ed.; Butterworth-Heinemann: Oxford, UK, 1992; pp 174−189.
(62) Israelachvili, J. N. *Intermolecular and Surface Forces*, 3rd ed.; Elsevier: Burlington, MA, 2011; pp 291−299.
(63) Gilman-Politi, R.; Harries, D. Unraveling the Molecular Mechanism of Enthalpy Driven Peptide Folding by Polyol Osmolytes. *J. Chem. Theory Comput.* **2011**, *60*, 4482−3828.
(64) Harries, D.; Rösgen, J. A Practical Guide on How Osmolytes Modulate Macromolecular Properties. In *Biophysical Tools for Biologists: Vol 1 in Vitro Techniques*; Elsevier Academic Press Inc.: New York, 2008; Vol. *84*, 679−735.
(65) Harries, D.; Rau, D. C.; Parsegian, V. A. Solutes Probe Hydration in Specific Association of Cyclodextrin and Adamantane. *J. Am. Chem. Soc.* **2005**, *127*, 2184−2190.
(66) Ghosh, T.; Kalra, A.; Garde, S. On the Salt-Induced Stabilization of Pair and Many-Body Hydrophobic Interactions. *J. Phys. Chem. B* **2005**, *109*, 642−651.
(67) Atkins, P.; De Paula, J. *Physical Chemistry*, 9th ed.; Oxford University Press: Oxford, UK, 2010; pp 168−169.
(68) Bernadó, P.; Blackledge, M.; Sancho, J. Sequence-Specific Solvent Accessibilities of Protein Residues in Unfolded Protein Ensembles. *Biophys. J.* **2006**, *91*, 4536−4543.
(69) Estrada, J.; Bernadó, P.; Blackledge, M.; Sancho, J. ProtSA: A Web Application for Calculating Sequence Specific Protein Solvent Accessibilities in the Unfolded Ensemble. *BMC Bioinf.* **2009**, *10*, 104.
(70) Razeto, A.; Galunsky, B.; Kasche, V.; Wilson, K. S.; Lamzin, V. S. High resolution structure of bovine alpha-chymotrypsin (pdb entry 1YPH), 2005. http://www.rcsb.org/ (accessed Mar 18, 2015).
(71) McPhalen, C. A.; James, M. N. Crystal and Molecular Structure of the Serine Proteinase Inhibitor CI-2 from Barley Seeds. *Biochemistry* **1987**, *26*, 261−269.
(72) Vijay-Kumar, S.; Bugg, C. E.; Cook, W. J. Structure of Ubiquitin Refined at 1.8 A Resolution. *J. Mol. Biol.* **1987**, *194*, 531−544.
(73) Pike, A. C.; Brew, K.; Acharya, K. R. Crystal Structures of Guinea-Pig, Goat and Bovine Alpha-Lactalbumin Highlight the Enhanced Conformational Flexibility of Regions That Are Significant for Its Action in Lactose Synthase. *Structure* **1996**, *4*, 691−703.
(74) Haynes, C. A.; Beynon, R. A.; Blanch, H. W.; Prausnitz, J. M. Thermodynamic Properties of Aqueous Polymer Solutions: Poly-(ethy1ene glycol)/Dextran. *J. Phys. Chem.* **1989**, *93*, 5612−5617.
(75) Eckelt, J.; Sugaya, R.; Wolf, B. A. Pullulan and Dextran: Uncommon Composition Dependent Flory-Huggins Interaction Parameters of Their Aqueous Solutions. *Biomacromolecules* **2008**, *9*, 1691−1697.
(76) Bercea, M.; Nichifor, M.; Eckelt, J.; Wolf, B. A. Dextran-Based Polycations: Thermodynamic Interaction with Water as Compared With Unsubstituted Dextran, 2 - Flory/Huggins Interaction Parameter. *Macromol. Chem. Phys.* **2011**, *212*, 1932−1940.
(77) Eliassi, A.; Modarress, H.; Mansoori, G. A. Measurement of Activity of Water in Aqueous Poly(ethylene Glycol) Solutions (Effect of Excess Volume on the Flory-Huggins Ø-Parameter). *J. Chem. Eng. Data* **1999**, *44*, 52−55.
(78) Canchi, D. R.; Paschek, D.; García, A. E. Equilibrium Study of Protein Denaturation by Urea. *J. Am. Chem. Soc.* **2010**, *132*, 2338−2344.
(79) Holthauzen, L. M. F.; Rösgen, J.; Bolen, D. W. Hydrogen Bonding Progressively Strengthens upon Transfer of the Protein Urea-

DOI: 10.1021/acs.jctc.5b00258
J. Chem. Theory Comput. 2015, 11, 3478−3490

Denatured State to Water and Protecting Osmolytes. *Biochemistry* **2010**, *49*, 1310−1318.
(80) Rodríguez-Ropero, F.; van der Vegt, N. F. A. Direct Osmolyte-Macromolecule Interactions Confer Entropic Stability to Folded States. *J. Phys. Chem. B* **2014**, *118*, 7327−7334.
(81) Heyda, J.; Muzdalo, A.; Dzubiella, J. Rationalizing Polymer Swelling and Collapse under Attractive Cosolvent Conditions. *Macromolecules* **2013**, *46*, 1231−1238.
(82) Mukherji, D.; Marques, C. M.; Kremer, K. Polymer Collapse in Miscible Good Solvents Is a Generic Phenomenon Driven by Preferential Adsorption. *Nat. Commun.* **2014**, *5*, 4882.
(83) Heyden, M.; Bründermann, E.; Heugen, U.; Niehues, G.; Leitner, D. M.; Havenith, M. Long-Range Influence of Carbohydrates on the Solvation Dynamics of Water–Answers from Terahertz Absorption Measurements and Molecular Modeling Simulations. *J. Am. Chem. Soc.* **2008**, *130*, 5773−5779.
(84) Verde, A. V.; Campen, R. K. Disaccharide Topology Induces Slowdown in Local Water Dynamics. *J. Phys. Chem. B* **2011**, *115*, 7069−7084.
(85) Sajadi, M.; Berndt, F.; Richter, C.; Gerecke, M.; Mahrwald, R.; Ernsting, N. P. Observing the Hydration Layer of Trehalose with a Linked Molecular Terahertz Probe. *J. Phys. Chem. Lett.* **2014**, *5*, 1845−1849.
(86) Sapir, L.; Harries, D. Linking Trehalose Self-Association with Binary Aqueous Solution Equation of State. *J. Phys. Chem. B* **2011**, *115*, 624−634.
(87) Lerbret, A.; Bordat, P.; Affouard, F.; Descamps, M.; Migliardo, F. How Homogeneous Are the Trehalose, Maltose, and Sucrose Water Solutions? An Insight from Molecular Dynamics Simulations. *J. Phys. Chem. B* **2005**, *109*, 11046−11057.
(88) Stanley, C.; Rau, D. C. Preferential Hydration of DNA: The Magnitude and Distance Dependence of Alcohol and Polyol Interactions. *Biophys. J.* **2006**, *91*, 912−920.
(89) Politi, R.; Sapir, L.; Harries, D. The Impact of Polyols on Water Structure in Solution: A Computational Study. *J. Phys. Chem. A* **2009**, *113*, 7548−7555.
(90) Guo, F.; Friedman, J. M. Osmolyte-Induced Perturbations of Hydrogen Bonding between Hydration Layer Waters: Correlation with Protein Conformational Changes. *J. Phys. Chem. B* **2009**, *113*, 16632−16642.
(91) Towey, J. J.; Dougan, L. Structural Examination of the Impact of Glycerol on Water Structure. *J. Phys. Chem. B* **2012**, *116*, 1633−1641.
(92) Towey, J.; Soper, A.; Dougan, L. Molecular Insight into the Hydrogen Bonding and Micro-Segregation of a Cryoprotectant Molecule. *J. Phys. Chem. B* **2012**, *116*, 13898−13904.
(93) Badasyan, A.; Tonoyan, S. A.; Giacometti, A.; Podgornik, R.; Parsegian, V. A.; Mamasakhlisov, Y. S.; Morozov, V. F. Unified Description of Solvent Effects in the Helix-Coil Transition. *Phys. Rev. E* **2014**, *89*, 022723.
(94) Budkov, Y. A.; Kolesnikov, A. L.; Georgi, N.; Kiselev, M. G. A Statistical Theory of Cosolvent-Induced Coil-Globule Transitions in Dilute Polymer Solution. *J. Chem. Phys.* **2014**, *141*, 014902.
(95) Kumar, A.; Attri, P.; Venkatesu, P. Effect of Polyols on the Native Structure of A-Chymotrypsin: A Comparable Study. *Thermochim. Acta* **2012**, *536*, 55−62.
(96) Zhang, D.-L.; Wu, L.-J.; Chen, J.; Liang, Y. Effects of Macromolecular Crowding on the Structural Stability of Human A-Lactalbumin. *Acta Biochim. Biophys. Sin.* **2012**, *44*, 703−711.

DOI: 10.1021/acs.jctc.5b00258
J. Chem. Theory Comput. 2015, 11, 3478−3490